# UTILIZING HIGH PERFORMANCE SUPERCOMPUTING FACILITIES FOR INTERACTIVE THERMAL COMFORT ASSESSMENT

Christoph van Treeck[1], Petra Wenisch[1], Andre Borrmann[1],
Michael Pfaffinger[1], Nikola Cenic and Ernst Rank[1]

[1]Computational Civil and Environmental Engineering,
Technische Universität München, Arcisstr. 21, 80290 München, Germany

## ABSTRACT

We outline the current state of the development of a computational steering environment (CSE) for the interactive simulation and local assessment of indoor thermal comfort. The system consists of a parallel CFD kernel, a fast 3D mesh generator and a virtual reality-based visualization component. The numerical method is based on a lattice Boltzmann algorithm with extensions for simulations of turbulent convective flows. Utilizing high-performance supercomputing facilities, the CSE allows for modifying both the geometric model and the boundary conditions during runtime coupled with the immediate update of results. This is made possible by a space-tree based partitioning algorithm that facilitates the meshing of arbitrarily shaped, complex facet models in a matter of just a few seconds computing time.

Ongoing developments focus on the integration of a radiation solver, a human thermoregulation model and a local thermal comfort model. Our first step was therefore to develop a prototype for computing resultant surface temperatures mapped for the surface of a numerical manikin. Results are compared with measurement data.

## KEYWORDS

Thermal comfort, CFD, Computational Steering, Lattice Boltzmann, Virtual Reality, High-Performance Computing

## INTRODUCTION

The assessment of indoor thermal comfort is becoming increasingly important in the industrial environment. Relevant areas of application in this scope include

- the automotive industry,
- the aircraft industry,
- the railway/coach industry and
- the HVAC/building sector.

Besides thermal comfort and indoor air quality (physical health), the aspect of occupational safety can also play a role. Simulation provides a means of improving HVAC concepts in the early design stages of a product in particular and can thus help to shorten design cycles. Simulations such as computational fluid dynamics (CFD), finite element-based approaches or multi-zone building models, for example, are thereby state-of-the-art tools. Aspects that still require clarification by researchers and practitioners alike are the *integration* of simulation approaches

- in the sense of enhancing and coupling different mathematical/physical models and/or models at varying levels of detail (multi-physics problem) and
- with respect to linking tools with CAD systems, (building) product models or building information models (BIM).

As regards the increasing power and availability of computer hardware coupled with industrial efforts in terms of cost reduction, experiments and measurements for assessing thermal comfort in vehicles and rooms using thermal manikins will be increasingly replaced by numerical simulation using detailed thermal models.

Measurements by thermal manikins in combination with interviews of test persons exposed to specific ambient conditions are, however, necessary in order to relate surface and body core temperatures to human temperature sensation and thermal comfort perception. For vehicles, the ergonomic requirements of the thermal environment are described in ISO 14505, for example.

As opposed to popular models that record the steady-state human heat balance for the body as a whole and near thermal neutrality, a detailed numerical model for comfort assessment essentially consists of the following components:

- a flow and thermal radiation solver,
- a numerical thermal manikin modeling the heat exchange between the body and environment with a (passive) system taking physical and physiological properties, the blood circulation and the (active) human thermoregulation system into consideration,
- a model for the local and global temperature sensation, and
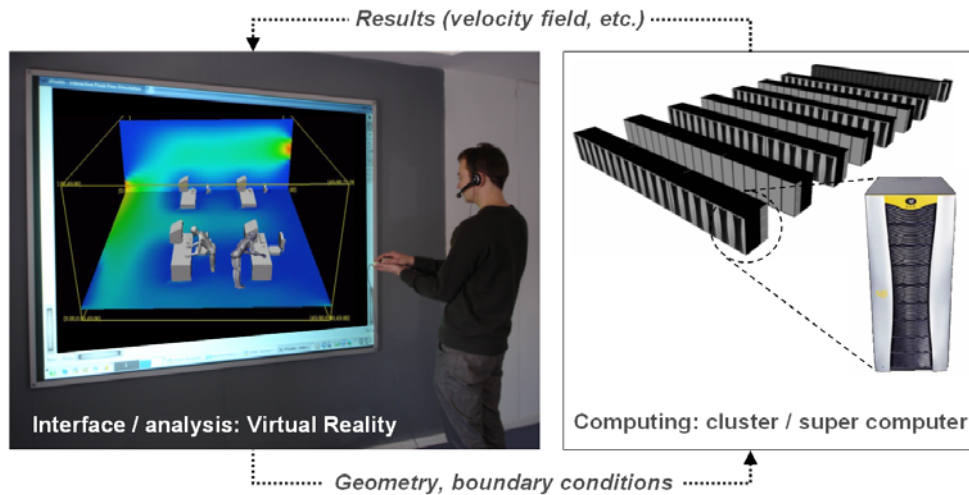- a model for thermal comfort assessment.

*Figure 1: Basic principle of computational steering: Modifications of geometry and/or boundary conditions are sent to the supercomputer; after remeshing and updating, new results are communicated back to the interactive VR environment for (stereoscopic) visualization. The example shows the air flow within an open plan office.*

Limited by the complexity of mesh generation and the effort for setting up numerical models of such coupled simulations, the application of these tools is clearly restricted.

In order to improve this situation, we outline the concept and the current status of a *computational steering environment (CSE)*, which is an interactive CFD environment allowing for local thermal comfort analysis by using high-performance supercomputing facilities and virtual reality techniques. The tools described in this paper make it possible to adapt both the boundary conditions and the geometric model and modify them during the simulation runtime with the immediate visualization of changes in the results.

Further simulations can be posted at a later date for certain configurations by way of batch jobs for detailed studies in non-interactive mode using enhanced physical models with a higher spatial resolution.

## ASSOCIATED RESEARCH PROJECTS

The CSE developments presented in this paper are the result of several research projects (Wenisch et al. 2004, van Treeck et al. 2006) and the long-term cooperation with the industry partner SIEMENS AG, Corporate Technology. The CSE is described in detail in the next section.

A local thermal comfort model is currently under development as part of a joint project (COMFSIM 2006) with partners at the Fraunhofer Institute for Building Physics (IBP), Germany. The model will be integrated into the simulation environment for the online assessment of the climatic impact of a given scenario on a virtual person. In order to compute the resultant surface temperature (RST) on each segment of the virtual thermal manikin, a human thermo-regulation model will be used in a next step.

In another associated project, the computing kernel is currently being optimized for the new German national supercomputer SGI Altix 4700 (HLRB II) in order to satisfy the requirements for hardware performance and the physical resolution of interactive simulations. The system offers a shared memory based layout with cache coherent, non-uniform memory access (ccNUMA) and consists of 9728 processors (Montecito dual-core type), has a peak performance of 62.3 TFlop/s and 17.5 TByte main memory (LRZ 2007).

## COMPUTATIONAL STEERING

Computational steering means 'to interact with a simulation itself', see (Mulder et al. 1999), for instance, and is more than just repeating the steps of preprocessing, simulation and postprocessing for a series of parameters – or more than interactively postprocessing previously computed results. By changing the geometry and parameters during the execution of a simulation with an immediate update of the results, engineers can explore the effects of their interactions *online*.

**Components of the CSE**

Figure 1 shows the basic principle. Modifications are communicated to the supercomputer which re-meshes the model and computes updates of the velocity and temperature fields, respectively. The term *interactivity* is used here to mean modifying boundary conditions as well as inserting, removing, translating, transforming, rotating and scaling geometric objects during simulation. Objects may be parametric obstacles such as a desk, active components such as a heater or a human manikin. The CSE supports the loading of predefined

scenarios. In particular, the CSE consists of the following components:

- a parallel CFD code based on the hybrid thermal lattice Boltzmann method (Lallemand and Luo 2003) using a multiple-relaxation-time scheme (d'Humières 2002) with extensions for simulations of turbulent convective flows (van Treeck 2004),

- a fast space tree-based 3D mesh generator (Wenisch et al. 2004),

- an integrated, virtual reality-based visualization engine (Wenisch et al. 2006) and

- a short-latency communication interface between kernel and visualization front end (Wenisch 2005).

The system also provides extensions for supporting collaborative engineering applications, where multiple visualization clients can be attached and detached during simulation, as demonstrated by Borrmann (2006).

The left-hand side of Figure 1 shows the stereoscopic visualization system with rear projection locally installed at the institute. The visualization front end PC is connected to the supercomputer via Gigabit Ethernet.

**Interactive VR menu**

The context-based interactive 3D menu is displayed in Figure 2. With the VR menu, single parameters may be modified or components added to a scene. The direct manipulation of objects can be realized with the help of the relevant object's draggers and grips (see top-most object in Figure 4, for example).
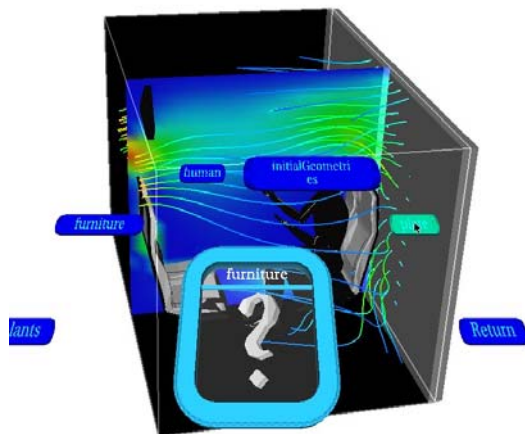


*Figure 2: Context-based VR menu*

**Software concept**

The CSE front-end is based on the OpenInventor library (Mercury 2006) and supports VR environments with single or multiple projection screens and input device tracking. In order to realize an event-driven communication concept, a simulation master node interacts with a set of computational nodes where the communication between the latter slave nodes is achieved using vendor-optimized MPI libraries. The concept is detailed in (Wenisch et al. 2006).

## MESH GENERATION

Besides the efficiency of the numerical kernel, fast and fully automated grid generation capabilities are required for interactive simulations with updates in sub-second time frames. We therefore use a hierarchic space-tree partitioning algorithm (Wenisch et al. 2004) in oder to create a digital voxel model with uniform grid spacing for the numerical scheme.
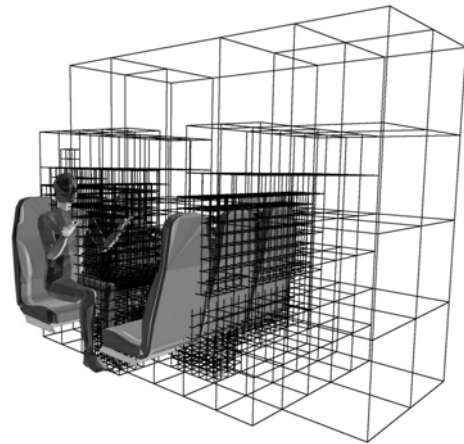


*Figure 3: Octree model of train model compartment*

A facet model based on the STL (stereo lithography) file format, which may be obtained using common CAD software, serves as the initial geometry. For grouping objects and setting up boundary conditions (which can also be done online later on within the CSE), a preprocessing tool has been integrated into the visualization tool Amira (Kollinger 2007).
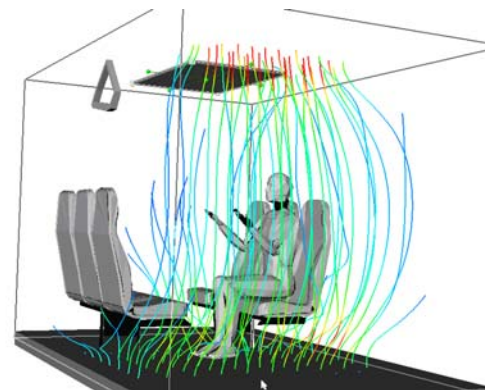


*Figure 4: Streamline visualization of cabin air flow*

The grid generator software allows the meshing of arbitrarily shaped, complex facet models in a matter of just a few seconds computing time. We wish to point out that the algorithm is also applicable even if

the model is geometrically inconsistent, i.e. if there are small gaps between facets. The example of the train compartment shown in Figure 3 was meshed in less than one second computing time on a single CPU. To improve this situation still further, the algorithm is parallelized using OpenMP, see (Wenisch et al. 2006).

## NUMERICAL METHOD

The numerical method applied in the parallel code is based on a hybrid thermal lattice Boltzmann (LB) scheme (Lallemand and Luo 2003) with extensions for simulations of turbulent convective flows (van Treeck et al. 2006).

### Lattice Boltzmann method

The Lattice Boltzmann method is an efficient approach for solving various Navier Stokes-like fluid flow problems in engineering applications and is increasingly attracting the attention of the industry. The method is based on statistical physics and computes the advection and local collision of an ensemble of particle distribution functions $f$ with respect to the Boltzmann equation with linearized collision operator $\Omega$ and external forces $\vec{F}$ (Lallemand et al. 1999).

$$\frac{\partial f}{\partial t} + \vec{\xi}\,\frac{\partial f}{\partial \vec{x}} + \vec{F}\,\frac{\partial f}{\partial \vec{\xi}} = \Omega(f,f) \qquad (1)$$

It can be shown that the complex nature of the collision integral $\Omega(f,f)$ in the Boltzmann equation can be simplified to describing a relaxation process towards a Maxwellian equilibrium distribution function for each lattice site (Bhatnagar et al. 1954). The continuous Boltzmann equation is discretized with respect to its microscopic velocity space by selecting a finite set of distribution functions $f_i$ with discrete microscopic velocities $\vec{\xi}_i$. Restricting the approach to small Knudsen numbers, it is sufficient to use a small number of velocities for spanning the phase space for athermal schemes. The set of discrete Boltzmann equations is then discretized in space and time $(\vec{x},t)$ along the characteristics with a first-order finite difference scheme (Lallemand and Luo 1999) which leads to the lattice Boltzmann equations. It should be stressed that other numerical discretization schemes may also be applied for the last step. The collocation points are selected to obtain the correct hydrodynamic equations and ensure that the cells defined by the phase space discretization coincide with the numerical grid.

This method has several advantages. The athermal lattice Boltzmann scheme does not posses numerical viscosity; it allows for high local element Reynolds values and yields a quadratic convergence if appropriate boundary conditions are applied. The first-order discretization scheme of the microscopic

velocity space yields second-order accuracy in terms of time and space with respect to the macroscopic moments (Lallemand 1999). The approach is accordingly restricted to low Mach values and small Knudsen values. As the collision process is an inherent local operation, this method can be efficiently implemented on parallel hardware as previously demonstrated by the authors.

In the recent years, a number of improvements have been published such as multi-grid (Tölke et al. 1998) or adaptive schemes (Filippova and Hänel 1998, Geller et al. 2006), for example.

### Hybrid thermal model

A multiple-relaxation-time (MRT) lattice Boltzmann scheme (d'Humières et al. 2002) is used to solve the incompressible mass and momentum equations. The MRT scheme provides improved numerical stability over the single-time relaxation (BGK) model of Bhatnagar et al. (1954).

A finite difference scheme is applied for solving the diffusion-advection equation, as proposed by Lallemand and Luo (2003), in order to circumvent the numerical instabilities of thermal lattice Boltzmann models. Both numerical methods use the same uniform Cartesian grid with appropriate interpolation schemes at the boundaries. The coupling between the LB and the finite difference scheme is explicit, i.e. the solution of the energy equation is used to compute a buoyant force

$$F(\vec{x},t) = g\,\beta\,\Delta t\, T(\vec{x},t) \qquad (2)$$

in the sense of a Boussinesq approximation, where $g$ is the acceleration due to gravity, $\beta$ the volume expansion coefficient and $\Delta t$ is the LB time step. As described by the author in (van Treeck 2006), the time steps for both schemes are adjusted for reasons of stability. The temperature field is computed by satisfying

$$\left(T_{i,j,k}(t + \Delta t^{FD}) - T_{i,j,k}(t)\right)\big/\Delta t^{FD} \;=$$
$$-\vec{u}_{i,j,k}\nabla^{(h)}_{i,j,k}T_{i,j,k}(t) + \kappa\Delta^{(h)}_{i,j,k}T_{i,j,k}(t) \qquad (3)$$

for each lattice site $(i,j,k)$ with the velocity $\vec{u}$ and the thermal diffusivity $\kappa$. The finite difference stencils $\nabla^{(h)}_{i,j,k}$ and $\Delta^{(h)}_{i,j,k}$ are given in (van Treeck 2004). The code has been validated in respect of the critical Rayleigh value behavior and natural convection in a square cavity in 2D and 3D at various Rayleigh values in the laminar and turbulent range up to Ra=$5\times10^{10}$, with and without turbulence model (van Treeck 2004, 2006).

Another advantage of the method is the local availability of the components of the traceless stress tensor as nodal quantities within the MRT scheme. There is, therefore, no need to compute these compo-

nents explicitly from derivatives of the velocity fields obtained. It is straightforward to compute an eddy viscosity required for algebraic turbulence modeling (Krafczyk 2003) if the turbulence is assumed to be homogenous and isotropic. For high-resolution simulations, we accordingly use a large eddy model. The Navier-Stokes equations are considered in a volume-averaged manner with implicit filtering for suppressing the small unresolved scales. The deviatoric part of the additional subgrid scale stresses is modeled dissipatively according to Smagorinsky (1963) as turbulent viscosity, which is added to the molecular one. Details are given in (van Treeck et al. 2006).

## THERMAL COMFORT ASSESSMENT

For the assessment of thermal comfort the approach given in EN ISO 7730, which is based on the work of Fanger (1982), is often applied in practice. The model considers the stationary heat balance of the human body as a whole and statistically relates the predicted mean vote (PMV) to ambient conditions, where the metabolism and the level of clothing are taken into account. The model is applicable to homogenous, uniform and steady-state environments close to thermal neutrality. ISO 7730 also gives tolerance limits for draught risk, temperature stratification and asymmetric radiation. However, the model is not valid for inhomogeneous or transient conditions. Nor is it possible to transfer this model to individual parts of the body with regard to the local effects of clothing and activity.

We know from experiments that temperature sensation and perception of thermal comfort are related to the thermal state of the human body, as detected by thermoreceptors, and depend on skin and core *temperatures* rather than calorimetric values (Fiala 1998). The thermal state of the body is a composite of several thermophysical and thermo-regulatory processes with weighted influence of the individual body parts.

### Thermal manikin models

Detailed manikin models usually consist of a passive system dealing with physical and physiological properties, including the blood circulation and an active thermoregulation system for the afferent signals analysis (Stolwijk 1971). Local clothing parameters are taken into account and the response of the metabolism can be simulated over a wide range of ambient conditions.

Besides two-node models (Gagge 1973), multi-segment models are known which are founded on the early work of (Stolwijk 1971). Most models use a decomposition of the human body into layers and segments for the passive system which are in thermodynamic contact. The 8-segment model of Stolwijk (1971) has been enhanced by Gordon

(1974), Wissler (1985), Werner (1988), Fiala (1998) and Tanabe (2002).

An active thermoregulatory system captures the four essential human responses to thermal influences: vasoconstriction, vasodilatation, sweating and shivering. It integrates thermal stimuli of thermo-sensitive areas and formulates a balanced response to signals from cutaneous thermoreceptors and the hypothalamus. According to Stolwijk (1971) afferent signals are usually interpreted as error signals, i.e. the deviation from set-point temperatures and their derivatives.

Fiala (1998) evaluated several models from literature and published detailed physiological and thermo-physical parameters for model calibration. Fiala formulated algebraic expressions for modeling the nonlinear behaviour of the cybernetic active system, i.e. for describing the local autonomic effects and regulation by the central nervous system. These formulae were obtained by detailed regression analyses of published data from literature and express source terms that are required within the bioheat equation (Pennes 1948) of the passive model.

In order to numerically compute the heat exchange between body and environment in detail, a thermal manikin model is currently under development as part of our COMFSIM project which is based on the work of Fiala (1998) and Stolwijk (1971). The model will be integrated into the CSE environment in a next step.

### Thermal sensation and comfort assessment

By taking into account the metabolism and the local level of clothing etc. with a numerical manikin, it is possible to compute resultant skin surface and body core temperatures, which are required for finally assessing the temperature sensation and the level of thermal comfort. Zhang (2004), for example, recently developed a detailed mathematical model based on measurements and interviews with test persons for both local and global thermal sensation and comfort.

Within the COMFSIM project we are currently developing a model for the local assessment of thermal sensation and comfort in conjunction with partners from Fraunhofer IBP. We refer to further publications.

## RESULTANT SURF. TEMPERATURE

Prior to integrating a detailed thermoregulation model into the code, we conducted a preliminary study for computing resultant surface temperatures (RST) on the surface of a thermal dummy. We accordingly developed a postprocessing prototype (Cenic 2005) that computes RST values (Mayer 2000), which are mapped on the facets of the numerical dummy by assuming a constant heat flux emitted from its artificial skin.

**Space interpolation scheme**

In the hybrid thermal model, the same underlying Cartesian grid is chosen for the LB model as for the finite difference scheme for the convection-diffusion equation. In order to evaluate surface heat fluxes and heat transfer coefficients, an appropriate spatial interpolation scheme is applied at the boundaries.
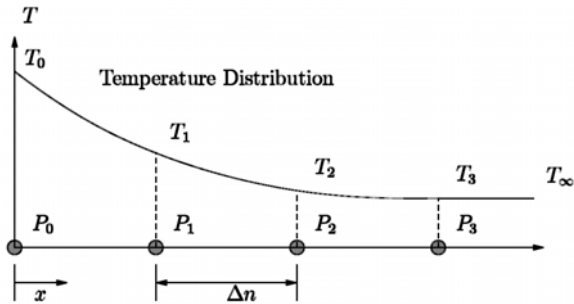


*Figure 5: Quadratic polynomial*

In order to compute the local derivatives of the normal temperature values for each facet, a quadratic polynomial is used, which is defined by the points $P_0$, $P_1$ and $P_2$ according to Figure 5. The interpolation points $P_i$ are obtained by trilinear interpolation in space, as shown in Figure 6 (the figure shows the 2D case only). As described in (Filippova 1998) or (van Treeck 2006), for example, depending on the position of the facet in space, an appropriate interpolation method must also be applied for curved boundaries (bounce back scheme) for the lattice Boltzmann scheme.
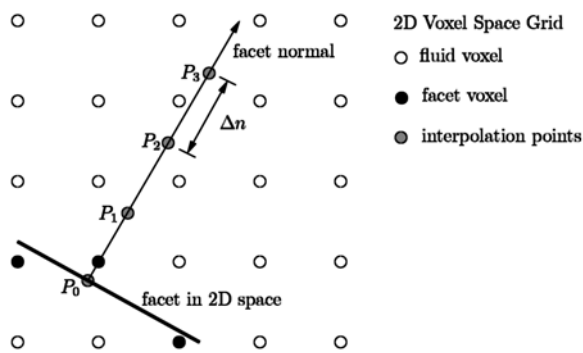


*Figure 6: Interpolation points $P_i$*

We are currently integrating the postprocessing module into our CSE for an online evaluation of heat fluxes and heat transfer coefficients.

## COMPARISON WITH MEASUREMENTS

Numerical results obtained from a LES simulation have been compared in a detailed study on measurement data in a testing facility provided by the Fraunhofer IBP. Details are given in (Cenic 2005).

**Experiment description**

The test room is air-tight, has a volume of 50m$^3$ and was equipped with two ventilation devices for creating a circulating air flow. Anemometers and sensors were available for measuring the wall surface temperatures. The room air and the wall temperatures were maintained at a constant level, incident short-wave radiation was eliminated in order to restrict the experiment to forced convection only. Figure 7 shows the basic room layout.
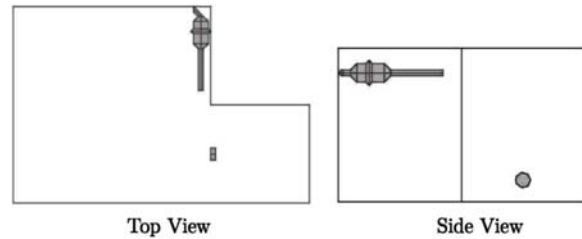


*Figure 7: Testing facility layout at IBP*

As indicated in Figure 8, the Fraunhofer thermal manikin DRESSMAN (Mayer 2000) was seated in the room. The dummy was equipped with several small, heated sensors on its artificial skin for measuring the resultant surface temperatures. RST values are obtained by relating the electrical resistance of the sensor to a calibration curve, cf. (Mayer 2000).
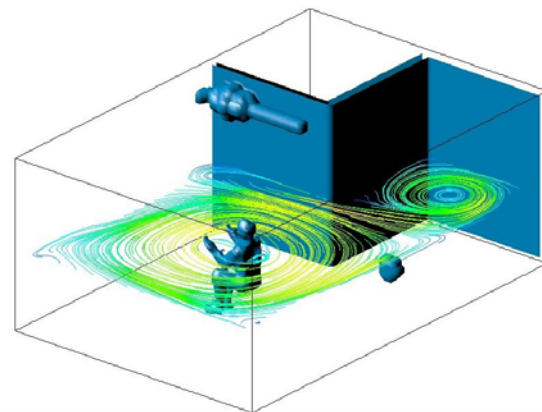


*Figure 8: Numerical simulation of convective flow, streamlines on slice plane of average velocity field*

**Numerical simulation**

Simulations were conducted in different mesh sizes using the hybrid scheme with the LES turbulence model. The local heating effect of the comparatively small temperature sensors was disregarded in the study by setting the surface temperature level on the dummy's surface to a constant value. Assuming a heat flux of $q=85$ $W/m^2$, as emitted from the heated sensors in the experiment, with the heat balance between skin and surroundings (Mayer 2000)

$$q = h_c(RST - T_\infty) + 4.9 \cdot 10^{-8} \left( RST^4 - T_{surf}^{\;\;4} \right) \qquad (4)$$

the RST values were computed using the Newton method for each facet, where $h_c$ is the convection heat transfer coefficient, $T_\infty$ the air temperature and $T_{surf}$ is the mean temperature of surrounding surfaces and values are given in [K]. With the fluid heat conductivity $\lambda$ the heat transfer coefficient

$$h_c = \frac{-\lambda(\partial T / \partial n)\big|_{n=0}}{T_0 - T_\infty} \qquad (5)$$

was accordingly obtained by evaluating the temperature gradient with the aforementioned interpolation scheme for each facet ($T_0$).

**Comparison with measurements**

Figure 9 shows the mapping of the RST values obtained on the surface of the thermal dummy model.
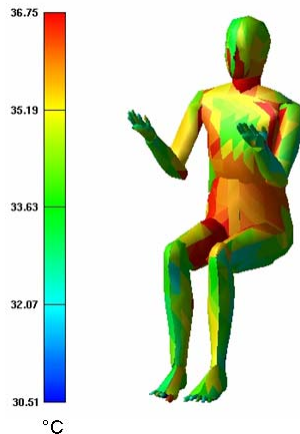


*Figure 9: Mapping of resultant surface temperatures (RST) on to the surface of the manikin*
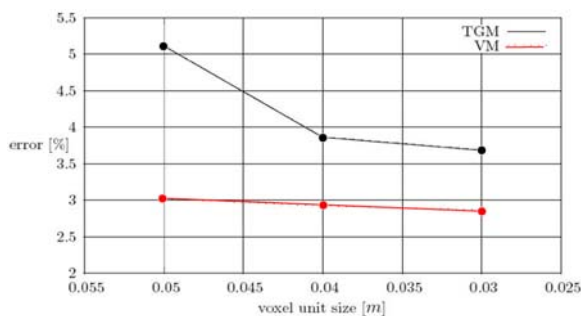


*Figure 10: Relative error between computed and measured RST values (see text for explanation)*

The computed RST values were compared with DRESSMAN measurements. The relative discrepancies between the computed and the measured RST values are plotted in Figure 10. In this figure, the method for evaluating the heat transfer coefficient according to eq. (5) is referred to as the temperature gradient method (TGM). VM indicates the use of an empirical method, referred to as the velocity method, where the convection heat transfer coefficient is empirically related to the air velocity for a fixed mean air temperature (Fanger 1982). The discrepancy is within a 5% tolerance and decreases with increasing accuracy, as expected. Further activities will include a detailed convergence study.

## CONCLUSIONS & FURTHER WORK

We have presented the latest developments of a computational steering environment (CSE) for interactive 3D CFD simulation using high-performance computers. The system consists of a parallel CFD kernel, a fast 3D mesh generator and a virtual, reality-based visualization component.

First numerical results on computing resultant surface temperatures on the surface of a thermal dummy model have been compared in a detailed study with measurement data. The developed postprocessing method is currently integrated in the CSE. Our main focus is finding on the most efficient way of implementing the spatial interpolation for maintaining fast response times of the kernel.

The next steps will be the implementation of a radiation solver, the integration of a detailed human thermoregulation model according to (Fiala 1998) and (Stolwijk 1971) and the development of a local thermal comfort model in collaboration with partners.

## ACKNOWLEDGEMENTS

## REFERENCES

Bhatnagar P., Gross E.P., Krook M.K. 1954. A model for collision processes in gases, Physical Review, 94(3): 511-525.

Borrmann A., Wenisch P., van Treeck C., Rank E. 2006. Collaborative comput. steering: Principles and appl. in HVAC layout, Integrated Computer-Aided Eng. (ICAE), vol. 13(4): 361-376.

Cenic N. 2005. Development of thermal comfort temperature sensors using CFD simulation based on LB methods, Master thesis, TU München.

Fanger P.O. 1982. Thermal comfort, Robert E. Krieger, Malabar.

Fiala D. 1998. Dynamische Simulation des menschlichen Wärmehaushalts und der thermischen Behaglichkeit, Dissertation, De Monfort University Leicester, HFT Stuttgart, Band 41.

Filippova O., Hänel D. 1998. Boundary-Fitting and Local Grid Refinement for LBGK Models, Int. J. Mod. Phys. C, 8, 1271-1279.

Gagge A. 1973. Rational temp. indices of man's thermal env. and their use with a 2-node model of his temp. reg. Fed. Proc., 32: 1572-1582.

Geller S., Tölke J., Krafczyk M. 2006. Lattice-Boltzmann Method on quadtree type grids for Fluid-Structure-Interaction. FSI: Modeling, Sim., Opt., In: H.-J. Bungartz and M. Schäfer, Springer.

Gordon R. 1974. The response of human thermoregulatory system in the cold. PhD thesis, Univ. of California, St. Barbara, CA.

d'Humières D., Ginzburg I., Krafczyk M., Lallemand P., Luo L.-S. 2002. MRT LB models in 3D, Phil. Trans. R. Soc. Lond. A, 360, 437-451.

Kollinger M. 2007. Definition strömungsmechanischer Randbedingungen für interaktive CFD Simulationen, Diploma thesis, TU München.

Krafczyk M., Tölke J., Luo L.-S. 2003. Large-eddy simulations with a multiple-relaxation-time LBE-model, Int. J. Modern Phys. B, 17: 33-39.

Lallemand P., Luo L.-S. 1999. Theory of the lattice Boltzmann method: Dispersion, dissipation, isotropy, Galilean invariance and stability, Physical Review E, 61(6): 6546-6562.

Lallemand P., Luo L.-S. 2003. Theory of the lattice Boltzmann method: Acoustic and thermal properties in two and three dimensions, Phys. Rev. E, 68, 036706.

LRZ. 2007. Leibniz Computing Centre of the Bavarian Academy of Sciences and Humanities, Germany, http://www.lrz-muenchen.de.

Mayer E. 2000. Manfitted measurement of thermal climate by a dummy representing suit for simulation of human heatloss (DRESSMAN), Healthy Buildings, Washington DC, 2: 551-556.

Mercury. 2006. OpenInventor, http://www.tgs.com.

Mulder J.D., van Wijk J.J., van Liere R. 1999. A survey of computational steering environments. Future Gener. Comput. Syst., 15(1): 119-129.

Pennes H. 1948. Analysis of tissue and arterial blood temperatures in the resting human forearm, J.Appl. Physiol., 1: 93-121.

Smagorinsky J. 1963. General circulation experiments with the primitive equations, I, The basic experiment, Mon. Weather Rev., 91, 99-165.

Stolwijk J.A.J. 1971. A mathematical model of physiol. temp. reg. in man, Tech. report, NASA CR-1855. Washington D.C.

Tanabe S.-I. et al. 2002. Eval. of thermal comfort using combined multinode thermoregulation (65MN) and radiation models and CFD. Energy and Buildings, 34: 637-646.

Tölke J., Krafczyk M., Schulz M., Rank E., Berrios R.. 1998. Implicit discretization and non-uniform mesh refinement approaches for FD discretizations of LBGK Models, Int. J. of Mod. Physics C, 9(8): 1143-1157.

van Treeck C. 2004. Gebäudemodell-basierte Simulation von Raumluftströmungen. PhD thesis, Technische Universität München.

van Treeck C., Rank E., Krafczyk M., Toelke J., Nachtwey B. 2006. Ext. of a hybrid thermal LBE scheme for Large-Eddy simulation of turb. conv. flows, Computers and Fluids, 35: 863-871.

van Treeck C., Rank E. 2006. ComfSim - Interaktive Strömungssimulation und lokale Komfortanalyse in Innenräumen. In: Bayerische Forschungsstiftung (Hrsg), Jahresbericht 2005, S.66, München.

Wenisch P., van Treeck C., Rank E. 2004. Interactive Indoor Air Flow Analysis using High Perf. Computing and VR Techn., Roomvent, Portugal.

Wenisch P., van Treeck C., Borrmann A., Rank E., Wenisch O. 2006. Comp. steering on distributed systems: indoor comfort sim. as a case study of interactive CFD on supercomp., Int. J. Parallel, Emergent and Distr. Systems, accepted for publ.

Wenisch P., Wenisch O., Rank E. 2005. Harnessing High-Perf. Comp. for Computational Steering, Lect. Notes in Comp. Sci.: Recent Adv. in Parallel Virtual Machine and Message Passing Interf., 3666: 536-543, Springer.

Werner J., Buse M. 1988. Temperature profiles with respect to inhomogenity and geometry of the human body, J. Appl. Physiol., 65(3):1110-1118.

Wissler E. 1985. Math. sim. of human thermal behaviour using whole body models. In: Shitzer, Eberhart: Heat Transf. in Med. and Biol., vol. 1, chap. 13: 325-373.

Zhang H., Huizenga C., Arens E., Wang D. 2004. Thermal sensation and comfort in transient non-uniform thermal environments, Eur. J. Appl. Physiol. 92: 728-733.